Biol Trace Elem Res (2018) 183:270–279
DOI 10.1007/s12011-017-1123-y

Organic Gallium Treatment Improves Osteoporotic Fracture Healing Through Affecting the OPG/RANKL Ratio and Expression of Serum Inflammatory Cytokines in Ovariectomized Rats

Jiashi Wang[1] · **Ming He**[1] · **Guangbin Wang**[1] · **Qin Fu**[1]

Received: 18 March 2017 / Accepted: 8 August 2017 / Published online: 24 August 2017

Abstract This study aimed to investigate the impact of organic gallium (OG) on osteoporotic fracture healing in ovariectomized female Sprague-Dawley rats, as well as study the mechanisms of OG on osteoporotic fracture healing. Forty-five female Sprague-Dawley rats were divided into three groups: sham operation group (Sxas control group), ovariectomized group (Ovx), and Ovx treated with OG group (Ovx + OG). Rat femoral fractures were studied using a standardized fracture-healing model utilizing bone fixation with an intramedullary pin. Six weeks later, analyses of micro-CT, histomorphometric, RNA extraction, RT-qPCR, and serum were performed following sacrifice of all mice. In comparison with Ovx group, OG can significantly increase bone volume (BV), tissue volume (TV), BV/TV radio, bone strength, callus bony area, and as similar to BMP-2 expression. OG treatment elevated OPG messenger RNA (mRNA) and inhibited RANKL mRNA, and showed an effect on OPG/RANKL ratio. OG treatment can inhibit the expression of TNF-α and IL-6. In conclusion, current study results indicate that organic OG can positively affect the OPG/RANKL ratio and inhibit the expression of serum inflammatory cytokines; thus, it can improve osteoporotic fracture healing.

✉ Qin Fu
doctorfuqin@sina.com

Jiashi Wang
wangjiashi2016@sina.com

Ming He
topheming56@163.com

Guangbin Wang
wanggb@sj-hospital.org

[1] Department of Orthopedic Surgery, Shengjing Hospital of China Medical University, 36 Sanhao Street, Heping District, Shenyang 110004, People's Republic of China

Keywords Gallium · Osteoporosis · Fracture healing · Inflammatory cytokine · OPG · RANKL

Introduction

Osteoporosis has become a critical medical problem; it is a disease which has the characteristics of bone tissue microstructure degenerative changes and low bone mass; it can lead to fragile bone and an increased incidence of fractures [1]. Depending on the etiology, it can be divided into primary and secondary types: primary osteoporosis includes senile and postmenopausal osteoporosis, and secondary osteoporosis consists of only a small proportion [2]. Ovarian rat model is the most commonly used postmenopausal osteoporotic animal model. The same mechanisms control gains in bone mass and losses, in young and aged rats and humans [3].

The most dangerous part of osteoporosis is fracture which could be caused by even minor trauma or daily activities, even in common sites like spine, hip, and distal forearm [4–10]. The process of fracture healing is complex and most of it remains unclear. Osteoporotic fracture healing process can significantly accelerate trabecular bone resorption; bone formation is slowed down by membrane bone formation and endochondral bone formation. Endochondral ossification delay; callus and callus collagen fibers within the loose arrangement are inconsistent with the main stress and healing strength. Osteoporotic fracture healing process has different characteristics in tissue, cell ultra-structure, many aspects of cytokines, and other mechanical properties compared with normal fracture healing.

Therapies used to treat osteoporosis (bisphosphonate, parathyroid hormone, vitamin D, estrogen) can interfere with fracture healing processes [11–15]. Paul Emile Lecoq de Boisbaudran first reported gallium (Ga) in 1875. It is an

element which shows semi-metallic properties; it can be used to treat tumor, resorptive, inflammatory, and immunosuppressive diseases [16–20]. Generally speaking, its anti-tumor functions were studied and have been shown to be effective in curing Paget's disease, hypercalcemia, and myeloma [21, 22]. As a potential bone resorption inhibitor, elemental gallium may treat osteoporosis and affect osteoporosis fracture healing process, but gallium also has side effects, which limit its use in treating osteoporosis [23–25]. On the contrary, organic gallium is a better choice since it can maintain effects but without strong gallium-related toxicity. Yeast can change it from an inorganic element to organic species which make it a good gallium carrier [26–28]. Thus, in this study, we mainly aim to explore yeast-incorporated gallium functions in osteoporotic fracture healing, as well as provide the mechanisms of it in osteoporotic fracture healing.

Materials and Methods

Organic Gallium

As described before [28], yeast cell lines (obtained from the Institute of Microbiology, Chinese Academy of Sciences) were implanted into a 125-ml Erlenmeyer flask which contained 30 ml YEPG medium (10 g yeast extract, 10 g peptone, 20 g glucose, and 3 g gallium nitrate per liter) and incubated for 20 h with rotary shaker (200 rpm at 28 °C). Gallium content was tested following cell harvest, and organic gallium (OG) was the yeast enriched in gallium. The gallium concentration in the yeast was tested using spectrophotometry, which was 471.2 ± 17.2 μg/g. The yeast enriched with gallium (OG) was dissolved in PBS to prepare a solution in which concentration of gallium was 20 μg/ml.

Animals and Fracture Model

Sprague-Dawley female rats (n = 45; weighing 234–290 g; 3-month-old; Beijing HFK Bioscience Co., Ltd.) were randomly allocated to three groups (15 rats/group): sham operation group (Sxas control group), ovariectomized group (Ovx), and Ovx treated with OG group (Ovx + OG) [3, 29]. All rats were housed 48% humidity and 20 °C constant temperature under 12-h dark/light cycles for 12 weeks. When rats were 24 weeks old, the osteoporosis of rats in Ovx group was measured at their lumbar vertebrae using dual-energy X-ray spectroscopy (DR-4500A; Hologic, MA, USA), which was applied to detect bone mineral density (BMD).

Experimental protocols were reviewed and approved by Chinese Legislation for animal usage. An injection of pentobarbitone sodium (40 mg/kg) was used to anesthetize rats. A closed femoral fracture model was developed with rats in both Sx and Ovx groups using intramedullary pins to stabilize the fracture. The fracture created was confirmed to be reproducible without observed infection.

Following surgery, Ovx rats were randomly allocated in equal numbers to Ovx + OG and Ovx + vehicle groups. Stomach lavaging to deliver OG and PBS was adopted for the study. After that, Sx and Ovx rats were treated with vehicle (PBS) through stomach lavaging, and Ovx + OG rats with yeast-bound gallium (at a gallium dosage of 120 μg/kg/day) for 6 weeks. Then all rats were sacrificed for micro-computed tomography (micro-CT), histomorphometric, RT-qPCR, and serum analysis.

Micro-computed Tomography Measurement

After sacrifice, all rat bone samples were measured using a micro-computed tomography (μCT) system (SCANCO Medical AG, Switzerland) and the results were analyzed using micro-view bone analysis software [3, 30]. Along femur length direction, whole length of the femur bone with fracture callus was scanned. Three hundred slices with thickness of 40 μm were then placed through the original fracture area. Fracture area was located at the site of center slice. To accurately match the region of interest (ROI) between all samples, we defined center fracture callus as formation of new bone tissue and original tissues were excluded. Eighty slices with thickness of 40 μm were then placed below and above the center fracture callous. Data were mainly focused on cortical thickness, outer callus, and marrow contour. The following parameters were recorded: tissue volume (TV), bone volume (BV), and BV/TV ratio, plus mean trabecular number (Tb.N), mean trabecular thickness (Tb.Th), and mean cortical thickness (Ct.Th).

After the micro-CT inspection, fractured femurs were fixed through transcardiac perfusion with 4% paraformaldehyde (Shanghai XinYu Biotech Co., Ltd.) in a phosphate buffer for 24 h at room temperature (RT) and decalcified using 10% EDTA (pH 7.4) for 28 days (medium was changed every 5 days) at RT, and then embedded in paraffin.

Hematoxylin-Eosin Staining

Each specimen longitudinally was sliced into 5-μm-thick slices, and the center section was chosen for analysis of each callus. Fractured femur tissue section was chosen and stained with hematoxylin and eosin (H&E) (Shanghai XinYu Biotech Co., Ltd.) for routine morphological analysis. Image-Pro 4.0 was used to measure bony area, total area of callus, and cartilage area.

Biomechanical Measurement

The rats' femoral neck mechanical strength was measured by the vertical pressure to load on the femoral head (Shimadzu

EZ-1, Osaka, Japan). Briefly, the rat femoral specimens were fixed with methyl methacrylate cement until the lesser trochanter to keep a vertical position. The vertical stress was done at the top of the femoral head from the cylinder. The direction of force is consistent with the long axis of the femoral shaft. The load was applied at an unchanging displacement rate of 2 mm/min until the rats' femoral neck fracture. The breakage load determined as the biomechanical characteristic of the bone was recorded at the peak force as Newton (N) at the point of the rat femoral neck fracture.

Immunohistochemical Staining for BMP-2 and Tartrate-Resistant Acid Phosphatase Staining

Immunohistochemistry for BMP-2 expression was assessed [31]. Serial 5-μm-thick sections were cut from the embedded specimens for immunohistochemical staining. Briefly, specific antibodies for BMP-2 (Abcam) were used for section immunohistochemistry staining overnight according to manufacturer's protocols to identify osteogenesis biomarkers. A goat anti-rabbit horseradish peroxidase (HRP) was used to verify the immunoreactivity in specimens. Following this, PBS (pH 7.4) was used for washing the sections. Results of immunoglobulin G (IgG) of isotype-matched control and primary antibody indicated background staining did not exist. Images of BMP-2 sections were captured using a high-resolution camera (Nikon DS-Fi1Nikon Corporation, Japan). The camera was linked to a microscope (OlympusBX-51, Japan) which was linked to a computer and results were analyzed with NIS-Elements software (Nikon Corporation, version 4.3). Relative areas of staining and optical density were respectively measured to determine BMP-2 expression.

To reveal osteoclasts, tissue sections were stained using tartrate-resistant acid phosphatase (TRAP), and any TRAP-positive multinucleated cell number was then calculated and was expressed as osteoclasts per millimeter of trabecular bone length.

RNA Extraction and rtPCR

A combination of liquid nitrogen and a bone tissue pulverizer (Shanghai XinYu Biotech Co., Ltd.) and RNeasy kit (Qiagen, Inc., Valencia, CA, USA) was used to crush left femurs to isolate RNA, according to the manufacturer's protocol. Reverse transcription was performed with the SuperScript® II Reverse Transcriptase kit (Invitrogen; Thermo Fisher Scientific, Inc.) according to the manufacturer's protocol. Subsequently, PCR was performed in order to assess the expression of messenger RNA (mRNA) using the GeneAmp® PCR System 9700 (Applied Biosystems; Thermo Fisher Scientific, Inc.) using PrimeSTAR HS DNA Polymerase with GC Buffer (Takara Bio, Dalian, China). Glyceraldehyde 3-phosphate dehydrogenase (GAPDH) was used as the internal loading control [32]. The primers were designed using Primer Premier 5.0 software (Premier Biosoft International, Palo Alto, CA, USA) and synthesized by Sangon Biotech Co. Ltd. (Shanghai, China) as follows:

OPG: forward 5′-TCCTGGCACCTACCTAAAACAGCA-3′; reverse 5′-CTACACTCTCGGCATTCACTTTGG-3′; RANKL: forward 5′-CACACCTCACCATCAATGCTGC-3′; reverse 5′-GAAGGGTTGGACACCTGAATGC-3′; BMP-2: forward 5′-CGTGAGGATTAGCAGGTCTTT-3′; reverse 5′-GGCGTTTCCGCTGTTTG-3′; RUNX2: forward 5′-TGCTGGAGTGATGTGGTTTTCT-3′; reverse 5′-CCCCTGTTGTGTTGTTTGGTAA-3′; ALP: forward 5′-CCGATGGCACACCTGCTT-3′; reverse 5′-GAGGCATACGCCATCACATG-3′; GAPDH: forward 5′-AGAAGGCTGGGGCTCATTTG-3′; reverse 5′-AGGGGCCATCCACAGTCTTC-3′

Stratagene Mx3000P software (Agilent Technologies, Inc., USA) was used to normalize mRNA to avoid housekeeping gene and GAPDH affect, and $2^{-\Delta\Delta Cq}$ method was used to calculate fold changes [33]. qPCR was conducted three times for each sample in order to measure the mean gene expression.

Western Blot

For Western blot analysis, the tissues were lysed using the RIPA buffer (Pierce, Rockford, IL, USA) in the presence of protease inhibitor cocktail (Pierce). Equivalent amounts of protein were resolved and mixed with 5X lane marker reducing sample buffer (Pierce), electrophoresed in a 10% SDS-acrylamide gel and transferred onto nitrocellulose membranes (Santa Cruz Biotechnology, USA). The membranes were blocked with 5% non-fat milk in Tris-buffered saline. Then the membranes were first probed by BMP-2 (sc-6267), RUNX2 (sc-8566), ALP (sc-365765), and GAPDH (sc-365062) antibody (SANTA, USA) and subsequently with HRP-conjugated secondary antibodies. Protein bands were visualized using enhanced chemiluminescence (ECL Western blotting detection, Amersham Life Science, Amersham, UK).

Measurement of TNF-α and IL-6 Level

Blood samples collected from dorsal aorta were centrifuged (3000*g* for 10 min) to collect serum (− 20 °C for preservation). TNF-α and IL-6 concentrations were measured using an ELISA kit (Shanghai XinYu Biotech Co., Ltd.). An IL-6- or TNF-α-specific monoclonal antibody was pre-coated onto a microplate. Samples and internal control antibodies were prepared into 96-well plates, and TNF-α and IL-6 were all bound to immobilize antibody. After unbound substances were washed away, TNF-α- or IL-6-specific polyclonal antibody was bound onto wells. Optical density was measured at 450 nm. Results were standardized using internal controls supplied with each kit.

Table 1 Bone structural variables of the femoral fracture calluses by micro-CT (mean ± standard deviation)

Groups	BV (mm)	TV (mm)	BV/TV (%)	Tb.Th (μm)	Tb.N (1/mm)	Ct.Th (μm)
Sx + vehicle	81.5 ± 9.7	226.6 ± 26.5	35.98 ± 3.4	104.5 ± 12.6	3.5 ± 0.4	272.6 ± 21.6
OVX + vehicle	64.8 ± 11.6*	203.1 ± 36.8*	31.9 ± 5.6*	87.0 ± 11.2*	2.9 ± 0.5*	240.3 ± 21.7*
OVX + OG	87.3 ± 12.7$^{\#}$	223.9 ± 32.1$^{\#}$	39.0 ± 3.1*,$^{\#}$	110.7 ± 14.4$^{\#}$	3.3 ± 0.4*,$^{\#}$	263.9 ± 27.3$^{\#}$

BV bone volume, *TV* tissue volume, *BV/TV* the ratio of bone volume to tissue volume, *Tb.Th* the mean trabecular thickness, *Tb.N* the mean trabecular number, *Ct.T* the mean cortical thickness

*$P < 0.05$ compared to Sx + vehicle; $^{\#}$ $P < 0.05$ compared to Ovx + vehicle

Data Analysis

All data were described as mean ± SD, SPSS 20.0 software (SPSS, Chicago, IL, USA) was used for analysis, and one-way ANOVA was used for comparisons between groups. Differences with P values of < 0.05 were considered to be significant.

Results

Effect of OG Treatment on BV, TV, BV/TV, Tb.Th, Tb.N, and Ct.Th of the Fractured Femurs

After 6 weeks of OG treatment, micro-CT results of fractured femur for BV, TV, BV/TV, Tb.Th, Tb.N, and Ct.Th (shown in Table 1) were recorded. In comparison with BV of Ovx + vehicle, BV of Ovx + OG showed an increase of 34.7% ($P < 0.05$). The BV/TV ratio of femoral fracture calluses in the Ovx + OG group was significantly increased by 22.3 and 8.6% in comparison with Ovx + vehicle and Sx + vehicle, respectively. Trabecular thickness (Tb.Th) of Ovx + OG group showed a significant increase of 27.2% in comparison with the Ovx + vehicle group. However, Tb.N showed a decrease in the Ovx + OG group in comparison with the Sx + vehicle group. Although cortical thickness (Ct.Th) was decreased in the Ovx + OG group in comparison with Sx + vehicle group, the difference was not statistically significant.

OG Treatment Can Affect Bone Formation Morphology in Fractured Femurs

After sacrifice of animals, specimens of fractured femurs were collected to observe the histological changes using a light microscope. Rats' femur callus callous area was analyzed using histomorphometric parameters, and three to five sections were chosen in each callus region. Figure 1 shows the histopathological results of fractured femurs after H&E staining. Image-Pro 4.0 was used to measure callus bony area, cartilage area, and callus total area (Fig. 2). Compared with sham group, the callus bony area in Ovx + vehicle group was 10.7% lower ($P < 0.05$). Additionally, the callus total area in the Ovx + OG group was 10.2 and 22.7% (both $P < 0.05$) higher than the callous total areas in the Sx + vehicle and Ovx groups, respectively. The cartilage area of Ovx + vehicle group showed a significant increase in comparison with Sx + vehicle group ($P < 0.05$).

OG Treatment Can Affect Rat Femoral Neck Biomechanical Strength

After sacrifice of animals, specimens of femurs were collected to observe the biomechanical measurement. The breakage load was recorded at the peak force as Newton (N) at the point of the rat femoral neck fracture (Fig. 3). The mean maximal fracture load of femoral neck in Ovx + OG group was 29.1%

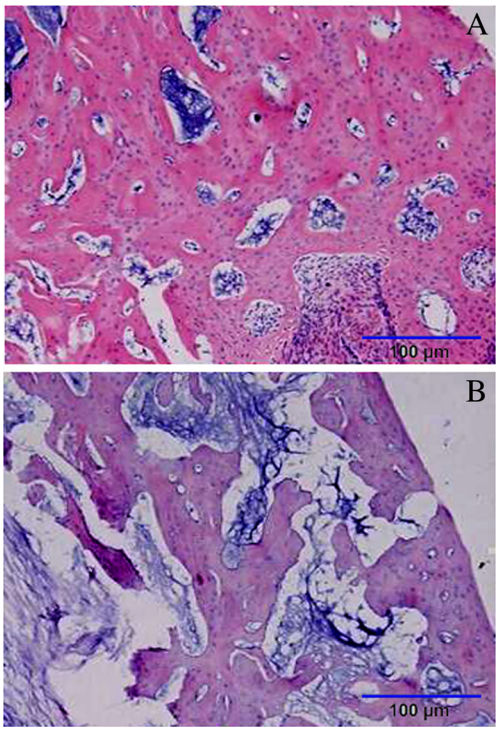

Fig. 1 H&E staining was used to observe fractured femur specimens under a light microscope. Histological appearance of callus zones OVX + OG group (**a**) and OVX + vehicle group (**b**). **a**, **b** Magnification × 40

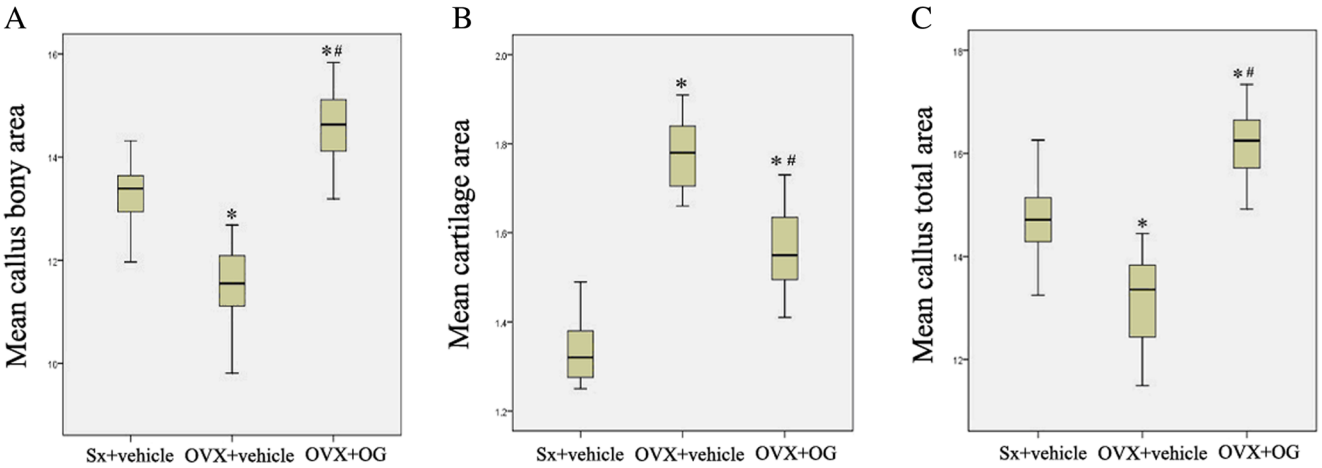

Fig. 2 OG affects bone formation histological morphology. Image-Pro 4.0 was used to measure callus bony area (**a**), cartilage area (**b**), and callus total area (**c**). Data were set as mean ± SD. $^{*}P < 0.05$ in comparison with Sx + vehicle; $^{\#}P < 0.05$ in comparison with OVX + vehicle

higher than that in Ovx + vehicle group ($P < 0.05$). The strength of femoral neck in Ovx + OG group was similar with Sx + vehicle group.

OG Treatment Does Not Affect BMP-2 Expression and Bone Formation in Fractured Femurs

The fractured femur sections were stained using immunohistochemistry to explore if OG treatment can affect BMP-2 expression [33] (Figs. 3 and 4a). The expression level of BMP-2 was detected using OD test and staining in relative area between the groups. After healing for 6 weeks, immunohistochemical staining showed BMP-2 expression in Ovx + OG group was similar to that of Ovx + vehicle ($P > 0.05$), but when compared with the Sx + vehicle group, a significant reduction was observed (Fig. 3, $P < 0.05$). After healing for 6 weeks, Western blot and real-time PCR showed the expression of BMP-2, RUNX2, and ALP in different groups. Results showed that Ovx + OG group was similar to that of Ovx + vehicle ($P > 0.05$), but when in comparison with Sx + vehicle, a significant reduction was observed (Fig. 4e, f, $P < 0.05$). From all the results above, we can conclude that OG treatment had no significant effects on bone formation.

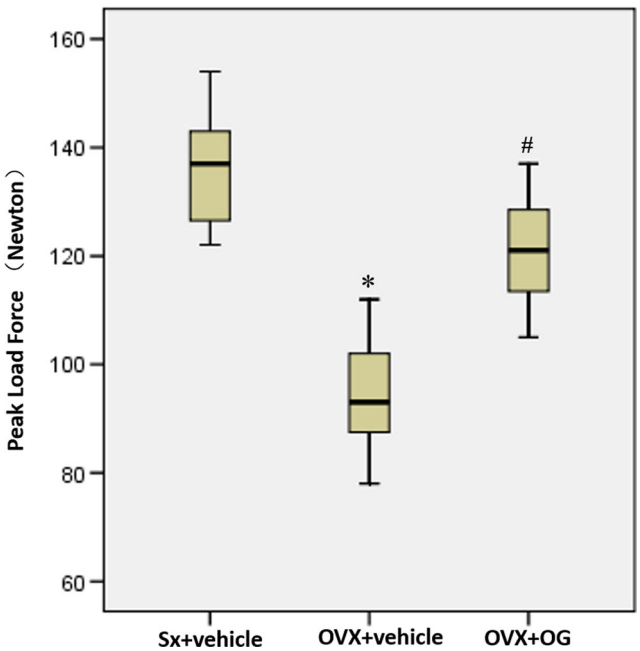

Fig. 3 OG treatment can affect rat femoral neck biomechanical strength. The breakage load was recorded at the peak force as Newton (N) at the point of the rat femoral neck fracture. Data were set as mean ± SD (N). $^{*}P < 0.05$ in comparison with Sx + vehicle; $^{\#}P < 0.05$ in comparison with OVX + vehicle

Effect of OG Treatment on Osteoclast Activity in the Fractured Femurs

After 6 weeks of healing, the fractured femur sections were stained with TRAP (Fig. 5) to verify the influence of OG treatment on osteoclast numbers. Only TRAP-positive multi-nucleated cells located in callus tissue were identified osteoclasts. In comparison with Ovx + vehicle, osteoclasts in callus tissue per square millimeter showed a significant decrease in the Ovx + OG group (32.6%, $P < 0.05$), indicating OG treatment can inhibit differentiation and function of osteoclast.

OG Treatment Affects OPG and RANKL mRNA in Fractured Femurs

OPG and RANKL mRNA expression was measured to explore the mechanism of OG regulation on osteoclast differentiation. As shown in Fig. 6, OG treatment increased OPG mRNA but decreased RANKL in the Ovx + OG group in comparison with the Ovx + vehicle group

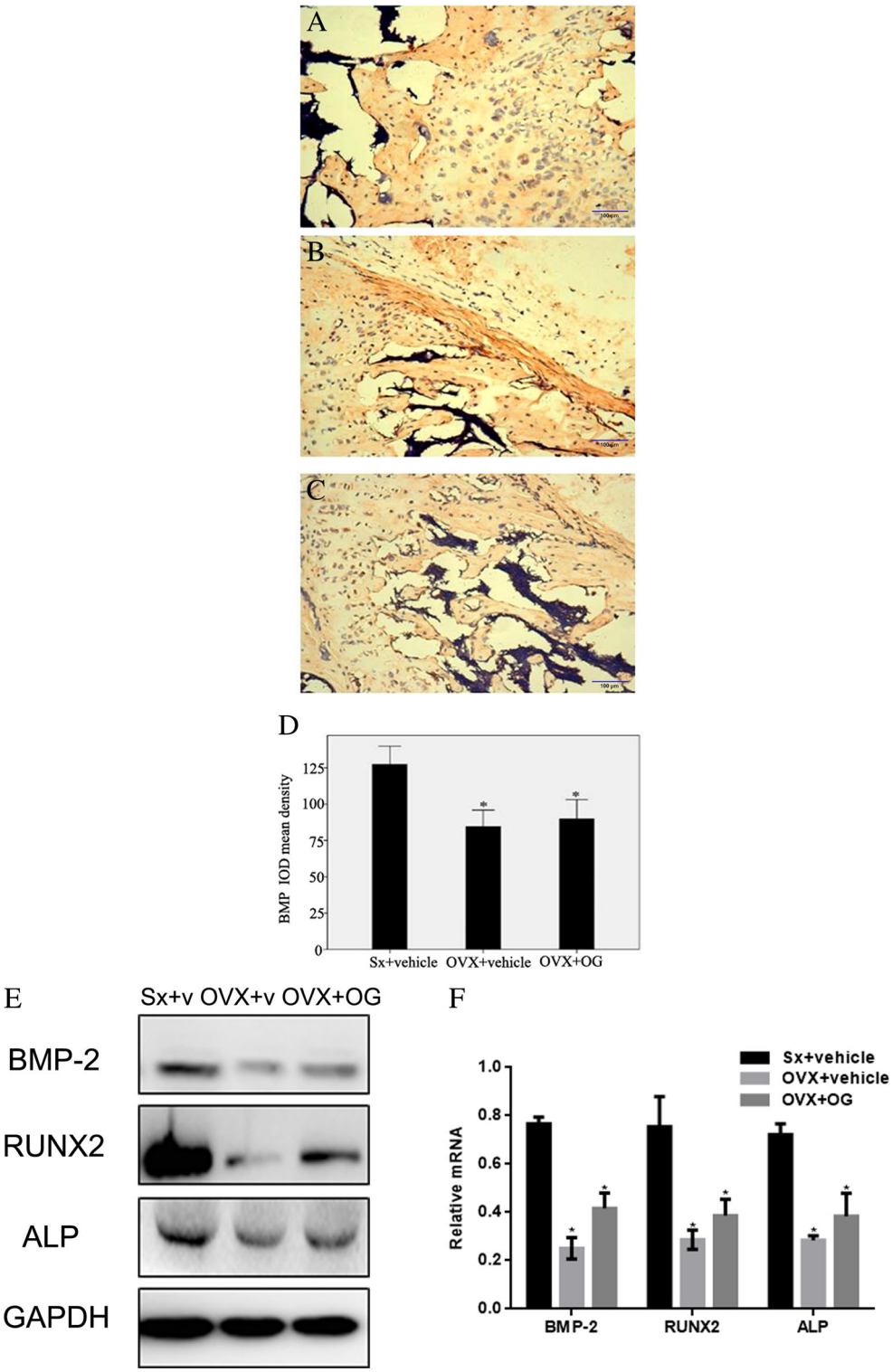

Fig. 4 OG treatment can affect BMP-2 expression. Immunohistochemistry appearance of BMP-2 in Sx + vehicle (**a**), OVX + vehicle (**b**), and OVX + OG group (**c**), and IOD BMP-2 expression mean density (**d**). Original magnifications of **a**, **b**, and **c** are × 40. Data were set as mean ± SD. $^{*}P < 0.05$ in comparison with Sx + vehicle; $^{\#}P < 0.05$ in comparison with OVX + vehicle. **a**, **b** Magnification × 40. **e**, **f** Western blot analysis and real-time PCR were performed to determine the expression of BMP-2, RUNX2, and ALP in different groups. $^{*}P < 0.05$ comparison with Sx + vehicle

($P < 0.05$), which demonstrated that OG can stimulate OPG expression and inhibit RANKL expression. This is in agreement with previous reports that showed OG can regulate osteoclast differentiation and function through affecting the OPG/RANKL mRNA expression ratio [34, 35].

OG Treatment Can Regulate Expression of Serum Inflammatory Cytokines TNF-α and IL-6 in the Fractured Femurs

OG treatment effects on TNF-α and IL-6 are shown in Fig. 7. In comparison with the Ovx + vehicle group, both IL-6 and

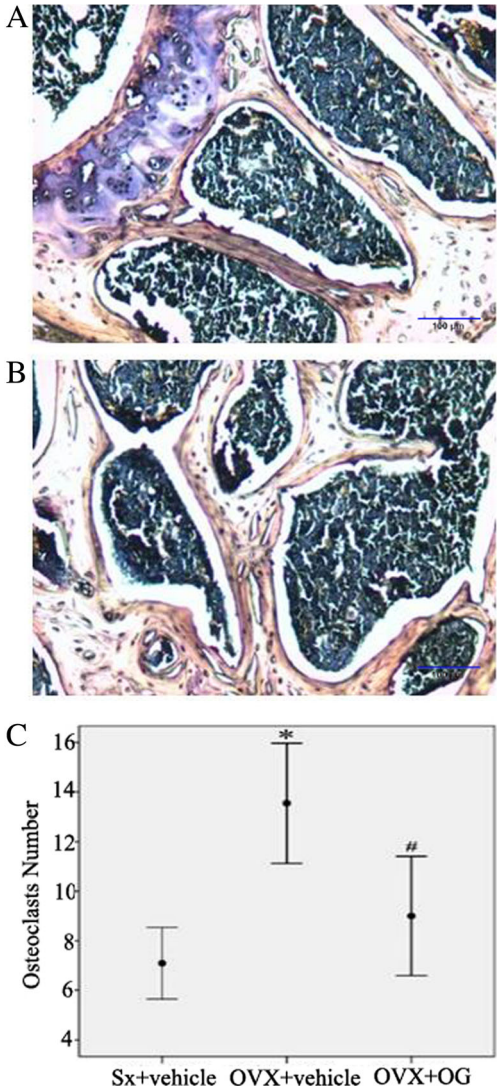

Fig. 5 OG treatment can affect osteoclast differentiation. TRAP staining appearance of osteoclast in OVX + vehicle group (**a**) and OVX + OG group (**b**). Mean osteoclast number in fracture callus section per square millimeter (**c**). Original magnifications of **a** and **b** are × 200. Data were set as mean ± SD. *$P < 0.05$ in comparison with Sx + vehicle; $^{\#}P < 0.05$ in comparison with OVX + vehicle

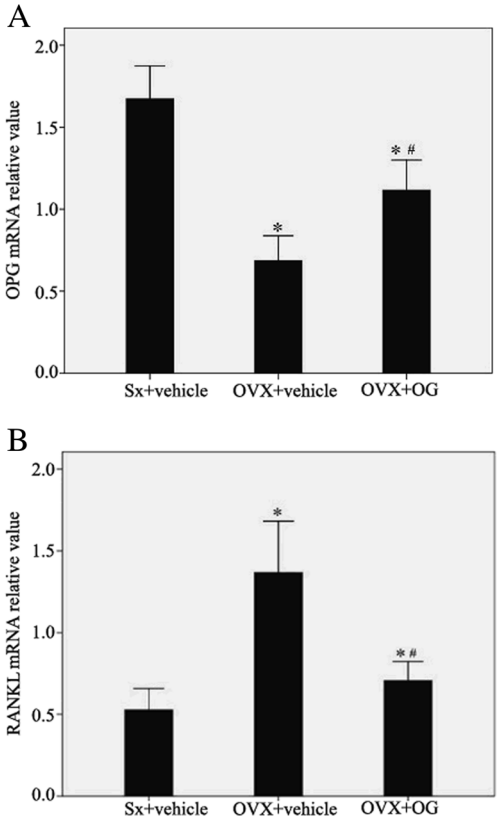

Fig. 6 OG treatment affects RANKL and OPG expression. The $2^{-\Delta\Delta Cq}$ method was used for data analysis. The OPG mRNA relative value (**a**) and the RANKL mRNA relative value (**b**). Data were set as mean ± SD. *$P < 0.05$ in comparison with Sx + vehicle; $^{\#}P < 0.05$ in comparison with OVX + vehicle

TNF-α showed lower levels in the Ovx + OG group ($P < 0.05$). IL-6 and TNF-α showed an increase in group Ovx + OG in comparison with group Sx + vehicle, but the difference was not statistically significant ($P > 0.05$). From all the results above, OG treatment inhibits TNF-α and IL-6 [35].

Discussion

Gallium (Ga) is an element which shows semi-metallic properties, and it can be used to treat tumor, resorptive, inflammatory, and immunosuppressive diseases [36]. As a potential inhibitor of bone resorption, elemental gallium may affect the osteoporotic fracture healing process [37]. Animal experimental results showed a reduction of serum mineral and an increase of bone mineral effect of yeast-incorporated gallium in ovariectomized osteopenic rats. However, no evidence of how OG influences osteoporotic fracture healing has been found. Thus, the current research primarily aims to explore mechanisms of OG in osteoporotic fracture healing.

Experimental results proved that OG treatment can increase callus bone volume, trabecular thickness, cortical thickness, and bony area in osteoporotic fractures in femurs of rats. There is a report showing that BV/TV is the best trabecular bone determinant and other morphological variables cannot do any further contribution [38, 39]. Thus, in osteoporotic fracture healing, an increase of callus parameter is of high importance in improving bone strength. In addition, OG treatment can increase the mean maximal fracture load of rat femoral neck in the experiment. Our data strongly suggest that OG can promote osteoporotic fracture healing.

BMP-2, expressed as the critical regulatory factor in the formation of bone tissue, belongs to the TGF-beta superfamily. BMP-2 is the only bone-derived BMP molecule which clearly can induce the entire cartilage and bone formation process by itself. There is increasing evidence that the BMP effects come from cooperation of a set of BMP-2-like

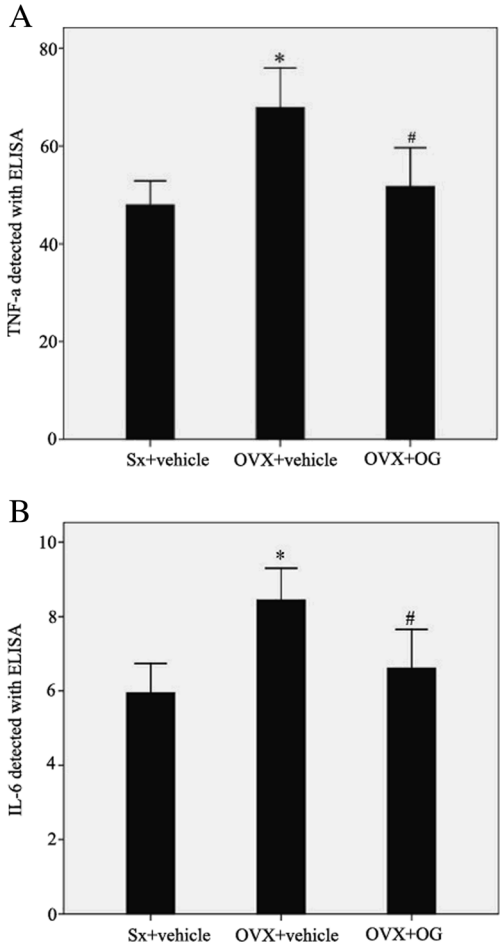

Fig. 7 Effect of OG on levels of the serum inflammatory cytokines TNF-α and IL-6. TNF-α level in serum (**a**) and IL-6 level in serum (**b**). Data were set as mean ± SD (pg/ml). *$P < 0.05$ in comparison with Sx + vehicle; $^{\#}P < 0.05$ in comparison with OVX + vehicle. TNF-α, tumor necrosis factor-α; IL-6, interleukin-6

molecules [40]. This current study demonstrated that the expression of BMP-2 was similar in the Ovx + OG group to OVX + vehicle, and osteoclast numbers showed a significant decrease in the Ovx + OG group in comparison with Ovx + vehicle group. Above all, these changes in bone properties which are mainly mediated through gallium were due to bone resorption suppression but not bone formation [40].

Osteoporotic fracture healing process normally proceeds in successive stages named the fracture, granulation, modeling, and remodeling stages. Osteoblasts and osteoclasts play a very important role in various stages of fracture healing.

Gallium has been shown an inhibitory action on both the differentiation and reabsorption activities of osteoclasts. However, the specific mechanism is not very clear. Hall et al. demonstrated that Ga inhibited activity of osteoclasts in a dose-dependent manner (100 μg/ml) [41], similar data was obtained by Verron et al. [42]. As noted by Strazic et al., gallium dose-dependently inhibited the tumor cell-induced osteoclastic differentiation of RAW 264.7 cells in vitro [43]. Verron et al. showed gallium considerably disturbed both the initial induction and the auto-amplification step of Nfatc1 gene, in the early stages of osteoclast differentiation. In addition, TRPV-5 calcium channel, which is located within the plasma membrane, is a target of Ga action on human osteoclast progenitor cells [42]. In the experiment, we also observed OG treatment can inhibit differentiation and function of osteoclast.

Few studies have showed the effect of gallium on osteoblast activity. Stern et al. demonstrated that gallium may enhance osteoclastic activity in osteopenia rats [44]. Jenis et al. showed that gallium induced an increase of collagen-1 gene expression and reduction of osteoclastic gene expression in osteoblast-like rat osteosarcoma cells and normal diploid rat osteoblasts in vitro [45]. The reason for this difference may be due to the dose of gallium and the environment in vitro and in vivo.

The main function of bones is to provide a framework to support the body and work with skeletal muscles, tendons, ligaments, and joints to allow movement. Bone formation and resorption of bone are commonly in homeostasis, ensuring maintenance of a stable bone mass. The homeostasis is mainly maintained through osteoblast and osteoclast cooperation [46]. Osteoprotegerin (OPG) is a protein with potential osteoclast genesis inhibitory activity that is naturally expressed in osteoblasts/stromal cells [47, 48]. RANKL, produced by osteoblasts/stromal cells, is a transmembrane ligand which can bind to RANK. RANKL/RANKL interaction can initiate a gene expression and signaling cascade which leads to osteoclast precursor cell differentiation and maturation to mature osteoclasts. As a decoy receptor, osteoprotegerin competitively binds to RANKL and can prevent binding of RANKL to RANK, further inhibiting osteoclast differentiation. Estrogen does not directly affect osteoclasts but suppresses osteoclast differentiation by regulating osteoblast and RANKL/OPG ratio. The RANKL/OPG ratio was used to determine osteoclast differentiation and function [48–50].

Results of this study showed that OG can regulate the OPG/RANKL ratio and inhibit osteoclast genesis. These results support that OG can regulate osteoclast differentiation and function through stimulating OPG expression and inhibiting RANKL expression, which suggests a possible mechanism that OG can prevent postmenopausal osteoporosis.

As potent bone resorption cytokines, IL-6and TNF-α can promote osteoclast formation, induce bone resorption, and affect the normal bone remodeling [51, 52]. TNF-α and IL-6, which are secreted by monocytes and macrophages, can function on osteoclast precursor cells, either directly or indirectly to differentiate them into osteoclasts which perform a primary role in bone resorption. TNF-α affects the OPG/RANKL/RANK system via prostaglandin E2, induces RANKL expression, reduces OPG expression, promotes

differentiation of osteoclast precursors, and activates mature osteoclast formation [53]. Choi et al. demonstrated that gallium nitrate reduced the serum levels of TNF-α, IL-6, and IFN-γ ($P < 0.05$) and the mRNA expression levels of these cytokines in joint tissues in type II collagen-induced arthritis in mice through its inhibition of the NF-κB pathway [54]. Makkonen et al. have studied that gallium inhibited dose-dependently the secretion of IL-6, TNF-α, and NO from the LPS-induced macrophage-like RAW 264 cells in vitro [55]. In addition, gallium inhibited serum TNF-α levels in nude mice bearing a canine adenocarcinoma model of hum oral hyperkalemia of malignancy [56]. Gallium has been shown to accumulate at inflammation sites and has shown anti-inflammatory and immunosuppressive activity, and this has been observed in human disease animal models [24]. IL-6 and TNF-α expression showed an increase in osteoporotic patients. In comparison with the Ovx group, expression of IL-6 and TNF-α in OG group was significantly suppressed with significant difference ($P < 0.05$). OG inhibited serum TNF-α and IL-6 levels to further reduce osteoclast formation and differentiation. Our data strongly suggest that OG can promote osteoporotic fracture healing.

Conclusions

In conclusion, the present study demonstrates that OG increases callus area and trabecular microstructure properties and can decrease the number of osteoclast in Ovx osteoporotic fracture in rats. OG stimulates OPG expression and inhibits RANKL expression, as well as affecting the OPG/RANKL ratio. OG can also inhibit the expression of serum inflammatory cytokines. OG can regulate osteoclast differentiation and functions by these mechanisms to improve osteoporotic fracture healing.

Acknowledgements This research was funded by the National Natural Science Foundation of China (No. 81070688).

Compliance with Ethical Standards Experimental protocols were reviewed and approved by Chinese Legislation for animal usage.

References

1. Marcus R (1996) Clinical review 76: the nature of osteoporosis. J Clin Endocrinol Metab 81:1–5
2. Cimaz R, Biggioggero M (2001) Osteoporosis. Curr Rheumatol Rep 3:365–370
3. Frost HM, Jee WS (1992) On the rat model of human osteopenias and osteoporoses. Bone and mineral 18:227–236
4. Lau EM, Cooper C (1996) The epidemiology of osteoporosis. The oriental perspective in a world context. Clinical orthopaedics and related research 65–74
5. Beattie K, Adachi J, Ioannidis G, Papaioannou A, Leslie WD, Grewal R, MacDermid J, Hodsman AB (2015) Estimating osteoporotic fracture risk following a wrist fracture: a tale of two systems. Arch Osteoporos 10:13
6. Vitali C, Gussoni G, Bianchi G et al (2015) High prevalence of fragility vertebral fractures in patients hospitalised in Internal Medicine Units. Results of the POINT (Prevalence of Osteoporosis in INTernal medicine) study. Bone 74:114–120
7. Bliuc D, Center JR (2016) Determinants of mortality risk following osteoporotic fractures. Curr Opin Rheumatol 28:413–419
8. Namkung-Matthai H, Appleyard R, Jansen J, Hao Lin J, Maastricht S, Swain M, Mason RS, Murrell GA, Diwan AD, Diamond T (2001) Osteoporosis influences the early period of fracture healing in a rat osteoporotic model. Bone 28:80–86
9. Thomas-John M, Codd MB, Manne S, Watts NB, Mongey AB (2009) Risk factors for the development of osteoporosis and osteoporotic fractures among older men. J Rheumatol 36:1947–1952
10. Lee JH, Cho SK, Han M, Lee S, Kim JY, Ryu JA, Choi YY, Bae SC, Sung YK (2014) Validity and role of vertebral fracture assessment in detecting prevalent vertebral fracture in patients with rheumatoid arthritis. Joint, bone, spine : revue du rhumatisme 81:149–153
11. Murphy CM, Schindeler A, Cantrill LC, Mikulec K, Peacock L, Little DG (2015) PTH(1-34) treatment increases bisphosphonate turnover in fracture repair in rats. Journal of bone and mineral research : the official journal of the American Society for Bone and Mineral Research 30:1022–1029
12. Boytsov N, Zhang X, Sugihara T, Taylor K, Swindle R (2015) Osteoporotic fractures and associated hospitalizations among patients treated with teriparatide compared to a matched cohort of patients not treated with teriparatide. Curr Med Res Opin 31:1665–1675
13. Hao Y, Wang X, Wang L, Lu Y, Mao Z, Ge S, Dai K (2015) Zoledronic acid suppresses callus remodeling but enhances callus strength in an osteoporotic rat model of fracture healing. Bone 81:702–711
14. Maier GS, Seeger JB, Horas K, Roth KE, Kurth AA, Maus U (2015) The prevalence of vitamin D deficiency in patients with vertebral fragility fractures. Bone Joint J 97-B:89–93
15. Cauley JA (2015) Estrogen and bone health in men and women. Steroids 99:11–15
16. Casper ES, Stanton GF, Sordillo PP, Parente R, Michaelson RA, Vinceguerra V (1985) Phase II trial of gallium nitrate in patients with advanced malignant melanoma. Cancer treatment reports 69:1019–1020
17. Straus DJ (2003) Gallium nitrate in the treatment of lymphoma. Semin Oncol 30:25–33
18. Collery P, Keppler B, Madoulet C, Desoize B (2002) Gallium in cancer treatment. Crit Rev Oncol Hematol 42:283–296
19. Donnelly R, Bockman RS, Doty SB, Boskey AL (1991) Bone particles from gallium-treated rats are resistant to resorption in vivo. Bone and mineral 12:167–179
20. Warrell RP, Jr., Bockman RS (1989) Gallium in the treatment of hypercalcemia and bone metastasis. Important Adv Oncol 205–220
21. Hughes S, Peel-White AL, Peterson CK (1992) Paget's disease of bone—current thinking and management. J Manip Physiol Ther 15:242–249
22. Warrell RP Jr, Bosco B, Weinerman S, Levine B, Lane J, Bockman RS (1990) Gallium nitrate for advanced Paget disease of bone: effectiveness and dose-response analysis. Ann Intern Med 113:847–851
23. Chitambar CR (2010) Medical applications and toxicities of gallium compounds. Int J Environ Res Public Health 7:2337–2361
24. Bernstein LR, Tanner T, Godfrey C, Noll B (2000) Chemistry and pharmacokinetics of gallium maltolate, a compound with high oral gallium bioavailability. Metal-Based Drugs 7:33–47

25. Han C, Yuan J, Wang Y, Li L (2006) Hypoglycemic activity of fermented mushroom of Coprinus comatus rich in vanadium. Journal of trace elements in medicine and biology : organ of the Society for Minerals and Trace Elements 20:191–196
26. Ma Z, Fu Q (2010) Therapeutic effect of organic gallium on ovariectomized osteopenic rats by decreased serum minerals and increased bone mineral content. Biol Trace Elem Res 133:342–349
27. Ma Z, Fu Q (2010) Comparison of the therapeutic effects of yeast-incorporated gallium with those of inorganic gallium on ovariectomized osteopenic rats. Biol Trace Elem Res 134:280–287
28. Pei Y, Fu Q (2011) Yeast-incorporated gallium promotes fracture healing by increasing callus bony area and improving trabecular microstructure on ovariectomized osteopenic rats. Biol Trace Elem Res 141:207–215
29. Kalu DN (1991) The ovariectomized rat model of postmenopausal bone loss. Bone and mineral 15:175–191
30. Stenstrom M, Olander B, Carlsson CA, Carlsson GA, Lehto-Axtelius D, Hakanson R (1998) The use of computed microtomography to monitor morphological changes in small animals. Applied radiation and isotopes : including data, instrumentation and methods for use in agriculture, industry and medicine 49: 565–570
31. Lehnerdt G, Unkel C, Metz KA, Jahnke K, Neumann A (2008) Immunohistochemical evidence of BMP-2, -4 and -7 activity in otospongiosis. Acta Otolaryngol 128:13–17
32. Shanmugarajan S, Tsuruga E, Swoboda KJ, Maria BL, Ries WL, Reddy SV (2009) Bone loss in survival motor neuron (Smn(−/−) SMN2) genetic mouse model of spinal muscular atrophy. J Pathol 219:52–60
33. Livak KJ, Schmittgen TD (2001) Analysis of relative gene expression data using real-time quantitative PCR and the 2(−Delta Delta C(T)) method. Methods 25:402–408
34. Lacey DL, Timms E, Tan HL et al (1998) Osteoprotegerin ligand is a cytokine that regulates osteoclast differentiation and activation. Cell 93:165–176
35. Filvaroff E, Derynck R (1998) Bone remodelling: a signalling system for osteoclast regulation. Current biology : CB 8:R679–R682
36. Kanis JA (1994) Assessment of fracture risk and its application to screening for postmenopausal osteoporosis: synopsis of a WHO report. WHO Study Group. Osteoporos Int 4:368–381
37. Verron E, Masson M, Khoshniat S et al (2010) Gallium modulates osteoclastic bone resorption in vitro without affecting osteoblasts. Br J Pharmacol 159:1681–1692
38. Maquer G, Musy SN, Wandel J, Gross T, Zysset PK (2015) Bone volume fraction and fabric anisotropy are better determinants of trabecular bone stiffness than other morphological variables. J Bone Miner Res: Official J Am Soc Bone Miner Res 30:1000–1008
39. Rath C, Baum T, Monetti R et al (2013) Scaling relations between trabecular bone volume fraction and microstructure at different skeletal sites. Bone 57:377–383
40. Wozney JM (1989) Bone morphogenetic proteins. Prog Growth Factor Res 1:267–280
41. Hall TJ, Chambers TJ (1990) Gallium inhibits bone resorption by a direct effect on osteoclasts. Bone Miner 8:211–216
42. Verron E, Loubat A, Carle GF, Vignes-Colombeix C, Strazic I, Guicheux J, Rochet N, Bouler JM, Scimeca JC (2012) Molecular effects of gallium on osteoclastic differentiation of mouse and human monocytes. Biochem Pharmacol 83:671–679
43. Strazic-Geljic I, Guberovic I, Didak B, Schmid-Antomarchi H, Schmid-Alliana A, Boukhechba F, Bouler JM, Scimeca JC, Verron E (2016) Gallium, a promising candidate to disrupt the vicious cycle driving osteolytic metastases. Biochem Pharmacol 116:11–21
44. Stern LS, Matkovic V, Weisbrode SE, Apseloff G, Shepard DR, Mays DC, Gerber N (1994) The effects of gallium nitrate on osteopenia induced by ovariectomy and a low-calcium diet in rats. Bone and mineral 25:59–69
45. Jenis LG, Waud CE, Stein GS, Lian JB, Baran DT (1993) Effect of gallium nitrate in vitro and in normal rats. J Cell Biochem 52:330–336
46. Udagawa N (2002) Mechanisms involved in bone resorption. Biogerontology 3:79–83
47. Udagawa N, Takahashi N, Yasuda H et al (2000) Osteoprotegerin produced by osteoblasts is an important regulator in osteoclast development and function. Endocrinology 141:3478–3484
48. Aubin JE, Bonnelye E (2000) Osteoprotegerin and its ligand: a new paradigm for regulation of osteoclastogenesis and bone resorption. Osteoporosis international : a journal established as result of cooperation between the European Foundation for Osteoporosis and the National Osteoporosis Foundation of the USA 11:905–913
49. Hofbauer LC, Kuhne CA, Viereck V (2004) The OPG/RANKL/RANK system in metabolic bone diseases. J Musculoskelet Neuronal Interact 4:268–275
50. Takayanagi H (2005) Mechanistic insight into osteoclast differentiation in osteoimmunology. J Mol Med 83:170–179
51. Wong PK, Quinn JM, Sims NA, van Nieuwenhuijze A, Campbell IK, Wicks IP (2006) Interleukin-6 modulates production of T lymphocyte-derived cytokines in antigen-induced arthritis and drives inflammation-induced osteoclastogenesis. Arthritis Rheum 54:158–168
52. Inanir A, Ozoran K, Tutkak H, Mermerci B (2004) The effects of calcitriol therapy on serum interleukin-1, interleukin-6 and tumour necrosis factor-alpha concentrations in post-menopausal patients with osteoporosis. J Int Med Res 32:570–582
53. Kwan Tat S, Padrines M, Theoleyre S, Heymann D, Fortun Y (2004) IL-6, RANKL, TNF-alpha/IL-1: interrelations in bone resorption pathophysiology. Cytokine Growth Factor Rev 15:49–60
54. Choi JH, Lee JH, Roh KH et al (2014) Gallium nitrate ameliorates type II collagen-induced arthritis in mice. Int Immunopharmacol 20:269–275
55. Makkonen N, Hirvonen MR, Savolainen K, Lapinjoki S, Monkkonen J (1995) The effect of free gallium and gallium in liposomes on cytokine and nitric oxide secretion from macrophage-like cells in vitro. Inflamm Res 44:523–528
56. Merryman JI, Capen CC, Rosol TJ (1994) Effects of gallium nitrate in nude mice bearing a canine adenocarcinoma (CAC-8) model of humoral hypercalcemia of malignancy. Journal of bone and mineral research : the official journal of the American Society for Bone and Mineral Research 9:725–732